The Arctic Oscillation signature in the wintertime geopotential height and temperature fields

David W. J. Thompson and John M. Wallace
Department of Atmospheric Sciences, University of Washington, Seattle

Published in Geophysical Research Letters
Vol. 25, No. 9, 1297-1300 (1998)

Abstract. The leading empirical orthogonal function of the wintertime sea-level pressure field is more strongly coupled to surface air temperature fluctuations over the Eurasian continent than the North Atlantic Oscillation (NAO). It resembles the NAO in many respects, but its primary center of action covers more of the Arctic, giving it a more zonally symmetric appearance. Coupled to strong fluctuations at the 50-hPa level on the intraseasonal, interannual, and interdecadal time scales, this “Arctic Oscillation” (AO) can be interpreted as the surface signature of modulations in the strength of the polar vortex aloft. It is proposed that the zonally asymmetric surface air temperature and mid-tropospheric circulation anomalies observed in association with the AO may be secondary baroclinic features induced by the land-sea contrasts. The same modal structure is mirrored in the pronounced trends in winter and springtime surface air temperature, sea-level pressure, and 50-hPa height over the past 30 years: parts of Eurasia have warmed by as much as several K, sea-level pressure over parts of the Arctic has fallen by 4 hPa, and the core of the lower stratospheric polar vortex has cooled by several K. These trends can be interpreted as the development of a systematic bias in one of the atmosphere’s dominant, naturally occurring modes of variability.

Introduction

There is a growing body of evidence indicating that the stratospheric polar vortex is implicated in some of the interannual and secular variability of climate at the earth’s surface. *Baldwin et al.* [1994], *Perlwitz and Graf* [1995] *Cheng and Dunkerton* [1995], and *Kitoh et al.* [1996] have all documented the existence of coupling between the strength of the nearly zonally symmetric polar night jet at the 50-hPa level and a more wavelike pattern reminiscent of the North Atlantic Oscillation (NAO) at the 500-hPa level. *Hurrell* [1995] has shown that the NAO modulates wintertime surface air temperature (SAT) over much of Eurasia: negative sea-level pressure (SLP) anomalies over Iceland and enhanced westerlies across the North Atlantic at 50˚N (i.e., the positive polarity of the NAO) are associated with positive SAT anomalies extending from Great Britain and Scandinavia far into Siberia. *Hurrell* [1996] went on to demonstrate that the upward trend in the NAO during the past 30 years accounts for much of the warming in SAT averaged over the domain poleward of 20˚N. *Kodera and Yamazaki* [1994], *Graf et al.* [1995], and *Kodera and Koide* [1997] have suggested the possibility of a dynamical linkage between the recent wintertime warming over Eurasia and a strengthening of the polar night jet and *Robock and Mao* [1992], *Graf et al.* [1994], and *Kodera* [1994] have invoked similar linkages to explain the observed positive SAT anomalies over Eurasia during the winters following major volcanic eruptions. In this short contribution we will offer our own analysis and interpretation of these relationships based on the datasets listed in Table 1.

Results

In this section we construct a three-dimensional picture of the primary mode of wintertime variability over the Northern Hemisphere working from the ground up. The primary field variable in the analysis is SLP (p), expressed in terms of the equivalent height of the 1000-hPa surface (Z_{1000}) above sea-level using the approximate relation $Z_{1000} = 8(p\text{-}1000)$ where Z_{1000} is expressed in meters and p in hPa.

As the reference variable we use the leading principal component of the wintertime (November-April) monthly mean SLP anomaly field over the domain poleward of 20°N, which accounts for 22% of the variance and is well separated from the other eigenvalues as per the criterion of *North et al.* [1982]. The associated loading vector or empirical orthogonal function (EOF) is shown in the lower right panel of Fig. 1. First identified by *Lorenz* [1951] in zonally averaged SLP data and subsequently by *Kutzbach* [1970], *Wallace and Gutzler* [1981], and *Trenberth and Paolino* [1981] in gridded data, this mode involves a seesaw between the Arctic basin and parts of the surrounding zonal ring. It is a robust pattern that dominates both the intraseasonal (month-to-month) and the interannual variability throughout the entire 98-year SLP record, as documented in Fig. 2. In seasonally averaged data for the past 30 years the Pacific center of action is partially obscured by interdecadal trends (discussed later). However this feature can be recovered by removing the linear trend from the data at each gridpoint before performing the EOF analysis (Fig. 2, right panel). Although this pattern incorporates many of the features of the NAO, its slightly larger horizontal scale and higher degree of zonal symmetry render it more analogous to the leading EOF of SLP in the Southern Hemisphere [*Rogers and van Loon,* 1982], and more like a surface signature of the polar vortex aloft. To distinguish the pattern in Fig. 1 from the more regional NAO we will herein refer to it as the Arctic Oscillation (AO) and the associated principal component time series as the AO index. This subtle distinction, first hinted at in the analysis of *Baldwin et al.* [1994], is essential for appreciating the strength of the linkages discussed in the following paragraphs.

The lower left panel of Fig. 1 shows wintertime monthly mean SAT anomalies over land regressed upon the AO index. The pattern is similar to Fig. 3 of *Hurrell* [1995], but the correlations in Table 2 indicate that the AO accounts for a substantially larger fraction of the variance of Northern Hemisphere SAT than the NAO.

Patterns derived by regressing wintertime monthly mean geopotential height fields onto the normalized AO index are also shown in Fig. 1, together with the corresponding "expansion coefficient time series" generated by projecting monthly fields upon the respective regression patterns and averaging them over winter seasons. The SLP and 50-hPa height patterns are remarkably similar and their expansion coefficient time series are strongly correlated, as indicated in Table 3. The 50-hPa pattern is indicative of fluctuations in the strength of the polar vortex (Fig. 3). This 50-hPa height regression pattern is virtually identical to the leading EOF of 50-hPa height shown in Fig. 4. In fact, a SLP pattern virtually identical to the leading EOF in Fig. 1 can be recovered in the inverse manner, by regressing SLP upon the leading principal component of 50-hPa height. The geopotential height anomalies at the 50-hPa level are almost five times as strong as the 1000-hPa height anomalies associated with this mode. Since the spatial patterns at the two levels are similar, it follows that energy density (the product of density and squared amplitude) is nearly invariant over this height range. Regression patterns based on subsequent EOFs of SLP (not shown) do not exhibit any upward amplification from the troposphere to the stratosphere.

The 500-hPa height pattern in Fig. 1 is the sum of the SLP (or 1000-hPa) pattern below it plus the 1000-500-hPa thickness pattern to the left of it. The features in the thickness field are more clearly reflected in the 500-hPa height field than in the more zonally symmetric SLP and 50-hPa height fields. It follows that the temperature anomalies in the 500-50-hPa layer must largely cancel those in the lower troposphere. This compensation is reflected in the pattern of tropopause pressure regressed upon the AO index (Fig. 1, upper left panel). The 1000-500-hPa thickness anomalies bear a strong resemblance to the SAT anomalies in the panel below. The inter-relationships between the various patterns shown in Fig. 1 are entirely consistent with the results of the previous studies cited in the Introduction, but our inclusion of the additional fields in the analysis reveals more clearly a three-dimensional modal structure consisting of two components: a deep equivalent barotropic signature extending high into the stratosphere and a tropospherically confined baroclinic signature. The equivalent barotropic signature is dominated by the zonally symmetric component, whereas the baroclinic signature is more wavelike. These two signatures are not separate modes, but components of a single modal structure, as evidenced by the high correlations between the AO index and the expansion coefficient time series of the 1000-500-hPa thickness and 500-hPa height patterns (Table 3).

The intraseasonal and the detrended interannual variability (not shown) exhibit virtually identical vertical structures. The coupling between the 50-hPa height and SLP fields is not as strong in the intraseasonal variability (Table 3), but it is no less statistically significant owing to the larger number of degrees of freedom. Both intraseasonal and interannual variability exhibit substantial upward amplification.

Figure 5 shows the AO index and the expansion coefficient time series of the SAT field in Fig. 1 for the more extended period of record 1900-1997. Strong coupling is evident between the AO and the time series of its attendant SAT field on the interannual timescale, and both time series exhibit a trend over the past 30 years with falling SLP over the Arctic and warming over Siberia. These trends are also clearly evident in Fig. 1.

Thirty-year (1968-1997) linear trend maps for wintertime averaged SAT, SLP, and 50-hPa height (Fig. 6) strongly resemble the modal structure depicted in Fig. 1, but for one notable disagreement: the 30-year SLP trend is negative over both the Arctic and the North Pacific, whereas in the modal structure in Fig. 1 the SLP anomalies in the two regions are of opposite sign. The pressure decreases over the North Pacific were large enough to cancel the weak center of action over the North Pacific in the leading EOF of the seasonal-mean SLP field during this period: hence the need for the removal of the linear trend to recover the AO pattern in the right panel of Fig. 2. ENSO-like interdecadal variability documented by *Trenberth and Hurrell* [1994] and *Zhang et al.* [1997] has contributed to this anomalous behavior in the Pacific sector. Despite this discrepancy, the spatial correlation between the SLP trend and the EOF in Fig. 1 is 0.77. The observed wintertime warming over Eurasia and the cooling over Labrador [*IPCC,* 1995], the persistent cyclonic surface wind anomalies over the Beaufort Gyre [*Walsh*, 1996], the increasing prevalence of the high index phase of the NAO [*Hurrell*, 1995], and the strengthening of the stratospheric polar night jet [*Graf et al*., 1995; *Kodera and Koide,* 1997] in recent years are all related to the deepening of the polar vortex from the earth's surface to the lower stratosphere. The nearly five-fold amplification of the geopotential height anomalies from the troposphere to the 50-hPa level implies that the lower stratosphere over the Arctic has cooled by several degrees. Not only are the spatial patterns of the trend similar to those associated with the year-to-year variability, the relative amplitudes of the trends of the three fields in Fig. 6 are also quite comparable to those in Fig. 1: in each case the 30-year trend amounts to about 1.25 standard deviations of the month-to-month variability. Hence, the observed trends can be viewed as a bias in a preferred mode of month-to-month variability.

Interpretation

Anecdotal evidence of deep vertical coupling in the wintertime polar vortex includes events such as the dramatic stratospheric warming of January 1977, which was accompanied by the formation of a strong surface anticyclone over the Arctic [*Quiroz*, 1977]. However it has not been until the relatively recent studies cited in the Introduction that convincing statistical evidence of this coupling has been forthcoming.

The analysis in the previous section confirms the existence of deep vertical coupling in the wintertime polar vortex and its relation to SAT anomalies over Eurasia and the Northwest Atlantic during an extended (November-April) winter season. Whereas the studies of *Baldwin et al.* [1994], *Perlwitz and Graf* [1995], *Cheng and Dunkerton* [1995] and *Kitoh et al.* [1996] have represented the tropospheric circulation in terms of the 500- or 850-hPa height fields, this study has emphasized the SLP field. We have shown that fluctuations in the intensity of the stratospheric circulation are linked to the leading EOF of SLP, a robust, quasi-zonally symmetric mode of variability that has received much less attention than the more wavelike teleconnection patterns that dominate the leading EOFs of the mid-tropospheric geopotential height field. This deep vertical coupling evidently prevails through a wide range of frequencies and it is simulated in recent modeling studies of *Kitoh et al*. [1996], *Kodera et al.* [1996], and *Volodin and Galin* [1998].

The strengthening of the polar vortex over the past 30 years, unrelated to any known tropospheric forcing, has led to speculation that anthropogenically induced temperature changes at stratospheric levels might somehow be responsible. Mindful of the numerous unsuccessful attempts to establish a dynamical basis for "downward control" of the tropospheric circulation, we are not convinced that the trends originate in the stratosphere. Nevertheless, it is of interest to consider the ways in which such a "top down" linkage could conceivably operate.

Kodera and Yamazaki [1994] and *Perlwitz and Graf* [1995] have hypothesized that the SAT anomalies over Eurasia and Labrador are induced by an anomalous mid-tropospheric planetary-wave pattern which develops in response to the intensification of the stratospheric polar vortex. Here we offer an alternative interpretation motivated by the three-dimensional modal structure depicted in Fig. 1, which is the only such mode that exhibits nearly constant energy density at levels ranging from the surface to the middle stratosphere. We hypothesize that strong coupling between troposphere and stratosphere is intrinsic to the dynamics of the zonally symmetric polar vortex; i.e., that under certain conditions, dynamical processes at stratospheric levels can affect the strength of the polar vortex all the way down to the earth's surface through the combined effects of an induced, thermally indirect mean meridional circulation analogous to the Ferrell cell and induced changes in the poleward eddy fluxes of zonal momentum at intermediate levels.

We further speculate that the tropospheric signature of these induced fluctuations would be zonally symmetric were it not for the existence of land-sea contrasts. A stronger zonal flow should advect more mild marine air into the interior of the continents, cold continental air over the western oceans, and increase the frequency of Atlantic cyclones tracking through the Kara Sea [*Rogers and Thompson*, 1995], thereby inducing a pattern of SAT anomalies much like that in Figs. 1 and 6. The mid-tropospheric planetary-wave pattern in Fig. 1 may be regarded as the hydrostatic signature of these temperature anomalies; we question whether it plays an essential role in the coupling with the stratosphere.

Concluding remarks

If the deepening of the wintertime polar vortex continues into the 21st century, it could have ramifications beyond the wide ranging (but thus far subtle) changes in surface climate discussed in this article and in *Hurrell* [1995]. For example:

- the weakening (and in time, perhaps even a reversal) of the wind-driven Beaufort Gyre could further reduce the extent and thickness of the Arctic pack ice [*McPhee et al.,* 1998],
- enhanced cooling and deep convection in the seas to the west of Greenland could continue to produce anomalously large volumes of Labrador Sea water [*Dickson et al.,* 1997],

- changes in ocean temperatures and sea-ice boundaries, in combination with the strengthening of the westerlies across the North Atlantic, could affect fisheries recruitment,
- changes in winter and spring precipitation patterns over Eurasia could affect soil moisture and vegetation during the subsequent growing season.

If the observed trends are anthropogenically induced, it remains to be to determined whether they are of stratospheric origin (a response to radiatively induced temperature changes due to greenhouse gases, as argued by *Perlwitz and Graf* [1995], or to CFC-induced ozone depletion) or whether they represent an unanticipated deep barotropic response of the polar vortex to greenhouse warming in the troposphere.

Acknowledgments. We would like to thank N.-C. Lau for pointing out the subtle, but important influence of the trend on the structure of the leading EOF of seasonal-mean SLP based on data for the past 30 years. Thanks also to J. Hurrell, P. Rhines, C. Deser, C. Leovy, R. Reed, A. Gettelman, and two anonymous reviewers for their helpful comments and suggestions, and to C. Gudmundson for preparing the manuscript. This work was supported by the National Science Foundation under grant 9215512, and by NOAA under a grant to the Hayes Center. This is JISAO contribution number 494.

References

Baldwin, M. P., X. Cheng and T. J. Dunkerton, Observed correlations between winter-mean tropospheric and stratospheric circulation anomalies, *Geophys. Res. Lett., 21*, 1141-1144, 1994.

Cheng, X., and T. J. Dunkerton, Orthogonal rotation of spatial patterns derived from singular value decomposition analysis, *J. Climate, 8*, 2631-2643, 1995.

Dickson, R. R., J. R. N. Lazier, J. Meincke, and P. B. Rhines, and J. Swift, Long-term coordinated changes in the convective activity of the North Atlantic, *Progress in Oceanography, 38,* 241-295, 1997.

Graf, H. -F., J. Perlwitz, and I. Kirchner, Northern Hemisphere tropospheric mid-latitude circulation after violent volcanic eruptions, *Contr. Atm. Phys., 67*, 3-13, 1994.

Graf, H. -F., J. Perlwitz, I. Kirchner, and I. Schult, Recent northern winter climate trends, ozone changes, and increased greenhouse forcing, *Contr. Atm. Phys., 68*, 233-248, 1995.

Hurrell, J. W., Decadal trends in the North Atlantic Oscillation: Regional temperatures and precipitation, *Science*, *269,* 676-679, 1995.

Hurrell, J. W., Influence of variations in extratropical wintertime teleconnections on Northern Hemisphere temperature, *Geophys. Res. Lett., 83*, 665-668, 1996.

Hurrell, J. W., and H. van Loon, Decadal variations in climate associated with the North Atlantic Oscillation, *Clim. Change, 36*, 301-326, 1997.

IPCC, *Climate Change 1995: The Science of Climate Change*, J. T. Houghton, F. G. Meira Filho, B. A. Callander, K. Maskell (Eds.), Cambridge Univ. Press, Cambridge, U. K., 1995.

Jones, P. D., Hemispheric surface air temperature variations: A reanalysis and update to 1993, *J. Climate*, 7, 1794-1802, 1994.

Kitoh, A., H. Koide, K. Kodera, S. Yukimoto and A. Noda, Interannual variability in the stratospheric-tropospheric circulation in a coupled ocean-atmosphere GCM, *Geophys. Res. Lett., 23*, 543-546, 1996.

Kodera, K., Influence of volcanic eruptions on the troposphere through stratospheric dynamical processes in the Northern Hemisphere winter, *J. Geophys. Res., 99*, 1273-1282, 1994.

Kodera, K., and K. Yamazaki, A possible influence of recent polar stratospheric coolings on the troposphere in the Northern Hemisphere winter, *Geophys. Res. Lett., 21*, 809-812, 1994.

Kodera, K., and H. Koide, Spatial and seasonal characteristics of recent decadal trends in the northern hemisphere troposphere and stratosphere, *J. Geophys. Res., 102*, 19433-19447, 1997.

Kodera, K., M. Chiba, H. Koide, A. Kitoh, and Y. Nikaidou, Interannual variability of the winter stratosphere and troposphere in the Northern Hemisphere, *J. Met. Soc. Japan, 74*, 365-382, 1996.

Kutzbach, J. E., Large-scale features of monthly mean Northern Hemisphere anomaly maps of sea-level pressure, *Mon. Wea. Rev., 98*, 708-716, 1970.

Lorenz, E. N., Seasonal and irregular variations of the Northern Hemisphere sea-level pressure profile, *J. Meteor., 8*, 52-59, 1951.

McPhee, M. G., T. P. Stanton, J. H. Morison, and D. G. Martinson, Freshening of the upper ocean in the Arctic: Is perennial sea ice disappearing?, *Geophys. Res. Lett.,* in press, 1998.

North, G. R., T. L. Bell, R. F. Cahalan, and F. J. Moeng, Sampling errors in the estimation of empirical orthogonal functions, *Mon. Wea. Rev., 110*, 699-706, 1982.

Parker, D. E., C. K. Folland, and M. Jackson, Marine surface temperature: observed variations and data requirements, *Climatic Change*, 31, 559-600, 1995.

Perlwitz, J., and H. -F. Graf, The statistical connection between tropospheric and stratospheric circulation of the Northern Hemisphere in winter, *J. Climate, 8*, 2281-2295, 1995.

Quiroz, R. S., Tropospheric-stratospheric polar vortex breakdown of January 1977, *Geophys. Res. Lett., 4,* 151-154, 1977.

Robock, A., and J. Mao, Winter warming from large volcanic eruptions, *Geophys. Res. Lett., 12,* 2405-2408, 1992.

Rogers, J. C., and H. van Loon, Spatial variability of sea level pressure and 500-mb height anomalies over the Southern Hemisphere, *Mon. Wea., Rev., 110*, 1375-1392, 1982.

Rogers, J. C., and E. -M. Thompson, Atlantic Arctic cyclones and the mild Siberian winters of the 1980s, *Geophys. Res. Lett.*, 22, 799-802, 1995.

Trenberth, K. E., and D. A. Paolino, Characteristic patterns of variability of sea level pressure in the Northern Hemisphere, *Mon. Wea. Rev., 109*, 1169-1189, 1981.

Trenberth, K. E., and J. W. Hurrell, Decadal atmospheric-ocean variations in the Pacific, *Climate Dyn., 9,* 303-309, 1994.

Volodin, E.M., and V. Ya. Galin, The nature of the Northern Hemisphere winter troposphere circulation response to observed ozone depletion in low stratosphere, *Quart. J. Roy. Met. Soc*., *124*, 1-30, 1998.

Wallace, J. M., and D. S. Gutzler, Teleconnections in the geopotential height field during the Northern Hemisphere winter, *Mon. Wea., Rev., 109*, 784-812, 1981.

Walsh, J. E., W. L. Chapman and T. L. Shy, Recent decrease of sea level pressure in the central Arctic, *J. Climate, 9* 480-486, 1996.

Zhang, Y., J. M. Wallace and D. S. Battisti, ENSO-like interdecadal variability: 1900-93, *J. Climate, 10*, 1004-1020, 1997.

Table 1. Datasets used in this study.

	Resolution	Period of record	Source
Surface air temperature (SAT)	5× 5	1900-6/1997	See *Jones* [1994] and *Parker et al.* [1995].
Sea level pressure (SLP)	5 × 5	1900-4/1997	NCAR Data Support Section
Geopotential height and tropopause pressure	2.5× 2.5	1958-6/1997	NCEP/NCAR Reanalysis via NOAA Climate Diagnostics Center

Table 2. Correlation statistics (r) for the NAO[a] and AO from 1900-1995 (Nov-April monthly values). r (NAO, AO) = 0.69.

	$T_{\text{NH Land}}$	$T_{\text{NH Land+Ocean}}$	T_{Eurasia}[b]
NAO	0.17	0.16	0.23
AO	0.39	0.36	0.55

[a] The normalized monthly mean sea level pressure (SLP) difference between Ponta Delgada, Azores and Stykkisholmur, Iceland.
[b] If Lisbon is substituted for the NAO Azores station (i.e., see *Hurrell and Van Loon*, 1997), and Dec-March means are used, then correlations with Eurasian mean SAT are 0.57 for the NAO and 0.65 for the AO.

Table 3. Correlations (r) with AO index (Nov-Apr 1958-97).

AO	Monthly	Interannual	Intraseasonal
Z_{500}	0.95	0.95	0.94
Z_{50}	0.63	0.80	0.53
T_{Eurasia}	0.62	0.77	0.53
Z_{500}-Z_{1000}	0.88	0.94	0.85

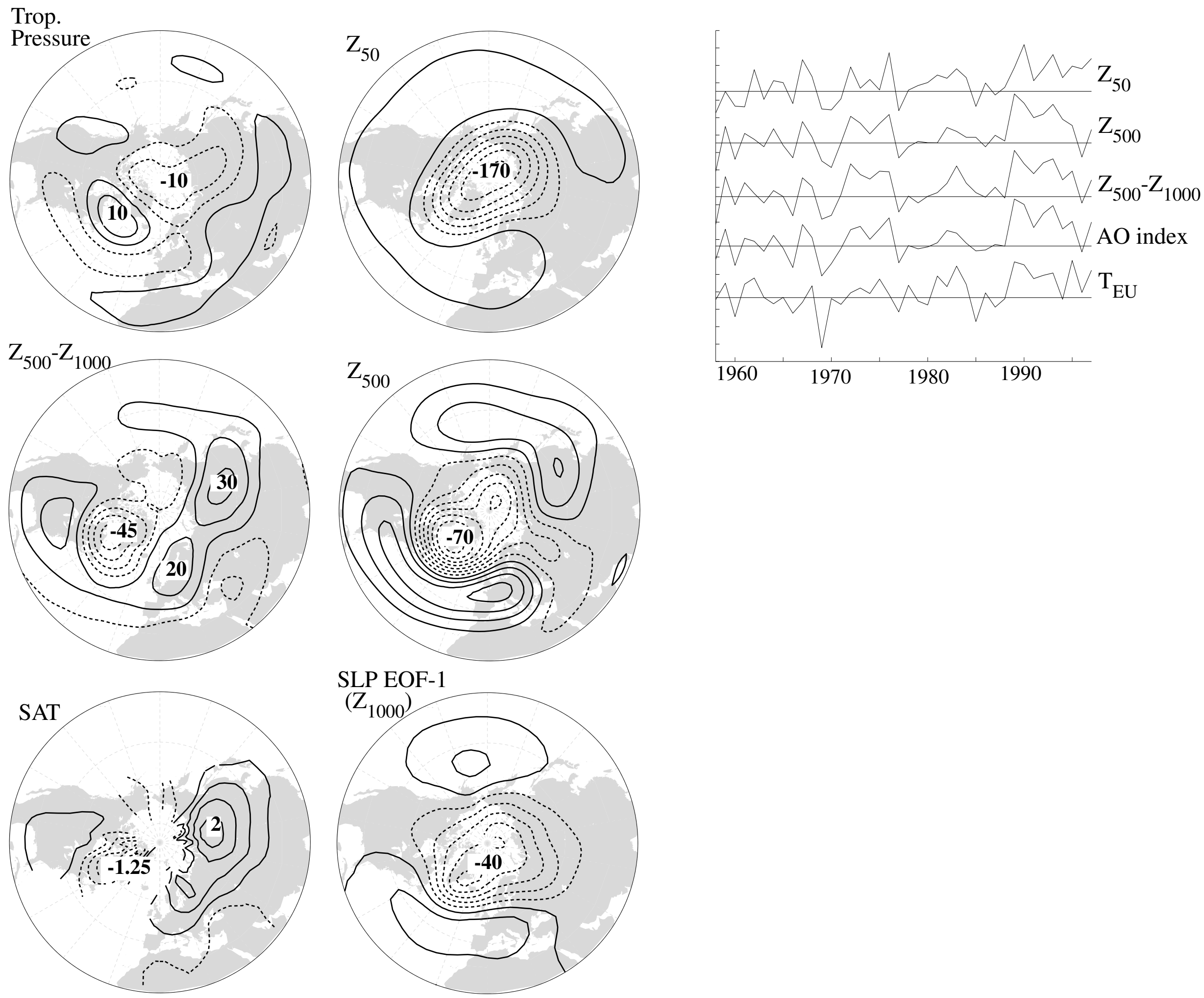

Figure 1. Left six panels: Regression maps for geopotential height (*Z*), tropopause pressure, 1000-500-hPa thickness and surface air temperature (SAT) anomalies, as indicated, based upon the leading principal component of wintertime (Nov-April) monthly mean sea-level pressure anomalies (the AO index) for 1947-1997. Contour intervals (expressed in units per standard deviation of the AO index) are: 10 m (-5, 5, 15...) for SLP (expressed as Z_{1000}), Z_{500}, and Z_{500}-Z_{1000}; 30 m (-45, -15, 15...) for Z_{50}; 5-hPa (-2.5, 2.5, 7.5...) for tropopause pressure; 0.5 K (-0.75, -0.25, 0.25...) for SAT. Negative contours are dashed. Extrema are labeled in the appropriate units. Top right, time series: (Top to bottom) Normalized expansion coefficient time series for the Z_{50}, Z_{500}, Z_{500}-Z_{1000}, and SLP regression maps depicted at left; normalized Eurasian mean (40 -70 N, 0 -140 E) SAT anomalies. Time series are wintertime (Nov-April) seasonal means based on monthly data from 1958-1997. Correlation statistics are presented in Table 3. Horizontal axes represent the means for years 1958-1967.

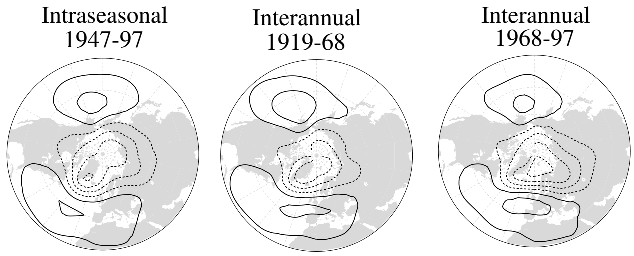

Figure 2. Left to right: Normalized leading EOFs of wintertime (Nov-April) SLP anomalies for: intraseasonal (month-to-month variability within winters) 1947-1997; seasonal averages 1919-1968; seasonal averages 1968-1997 detrended as described in text.

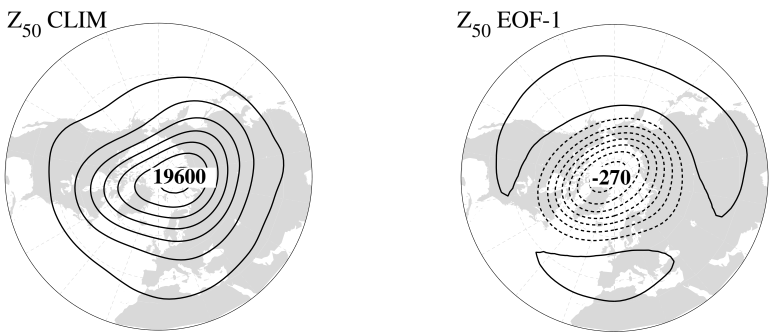

Figure 3 (left). Climatological wintertime (Nov-April) 50-hPa height field for 1958-1997. Contour interval is 150 m. **Figure 4 (right).** The leading EOF of wintertime 50-hPa geopotential height anomalies for 1958-1997, which accounts for 50% of the total variance. Contour interval 40 m (-60, -20, 20...). Negative contours are dashed.

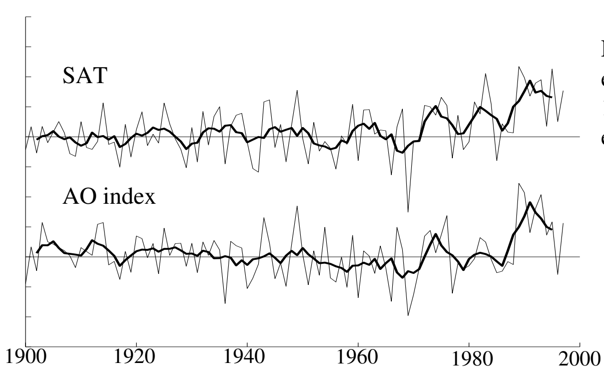

Figure 5. Top to bottom: Normalized wintertime expansion coefficient time series for the SAT and SLP regression maps of Fig. 1 for 1900-1997. The light lines denote unsmoothed seasonal averages ($r = 0.86$); heavy lines denote five-year running means.

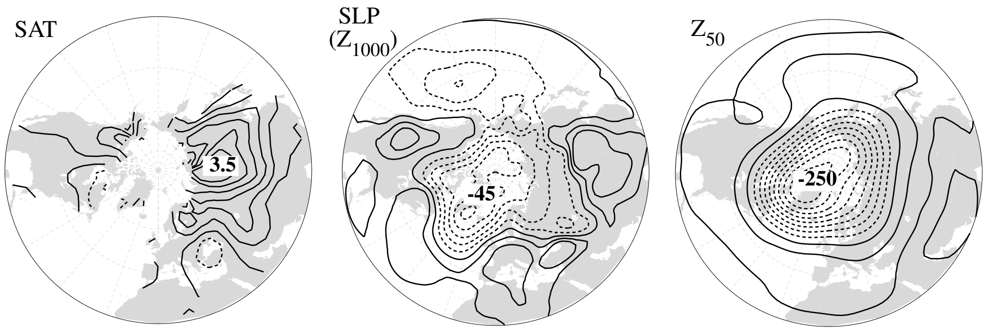

Figure 6. Left to right: 30-year (1968-1997) linear trends (as indicated) for: SAT anomalies; SLP (expressed as Z_{1000}) anomalies; 50-hPa geopotential height (*Z*) anomalies. All maps are based upon wintertime averaged (Nov-April) data. Contour intervals are (expressed in units per 30 years): 0.5 K (-0.25, 0.25, 0.75...) for SAT; 10 m (-15, -5, 5...) for Z_{1000}; 30m (-45, -15, 15...) for Z_{50}. Negative contours are dashed.